Original Research

Volume 5, Issue 2, pp 196-210, September, 2023

ACHIEVERS JOURNAL OF SCIENTIFIC RESEARCH

Open Access Publications of Achievers University, Owo

Available Online at *www.achieversjournalofscience.org*

Biosynthesis of Zinc Oxide Nanoparticles from Scent Leaf (*Ocimum gratissimum*) and Evaluation of its Antioxidant and Photocatalytic Activities

Ilesanmi, O.S.[1]*, Elijah, O.F. [1]and Kayode, A.B.[2]

[1] Department of Chemical Sciences (Biochemistry), Achievers University, Owo, Ondo State, Nigeria.

[2] Department of Fruit and Spices Research, National Horticultural Research Institute (NIHORT), Ibadan, Nigeria.

Corresponding author e-mail: osilesanmi@achievers.edu.ng; olutosinilesanmi@yahoo.com

Submitted: July 12, 2023, Revised: August 25, 2023, Accepted: September 02, 2023, Published: September 28, 2023

Abstract

Green synthesis of nanoparticles for several applications has gained attention in the field of science because of its cost-effectiveness and eco-friendliness. In this work, we synthesized zinc oxide nanoparticles (ZnO NPs) from scent leaf, characterized the synthesized nanoparticles and established its antioxidant and photocatalytic activities. The biosynthesized *O. gratissimum* zinc oxide nanoparticles (*Og*ZnO NPs) were analyzed. Thermal gravimetric analysis transition shows a loss of 12.65% up to 650°C, indicating that the *Og*ZnO NPs is thermally stable after 650°C. The patterns indicated crystalline orthogonal shape with a particle size of 15.5 nm. The Fourier transform infra-red spectroscopy of the synthesized *Og*ZnO NPs revealed different bands. The peak in the region of 650 cm^{-1} is assigned to Zn-O stretching vibration confirming formation of ZnO NPs. scanning electron microscope coupled with energy dispersive x-ray images and spectra revealed triangular crystalline shapes and presence of carbon and oxygen respectively. The percentage elemental compositions of the synthesized nanoparticles were 17.86%, 21.75%, 58.28%, 0.62% and 0.48% for carbon, oxygen, zinc, silver and nitrogen respectively . Strong absorption bands of the biosynthesized samples observed from UV-visible spectra at 350–400nm was characteristic band of ZnO nanoparticles. Free radical scavenging activity of the synthesized *Og*ZnO NPs revealed that it possesses high antioxidant property in a concentration dependent manner. The photocatalytic activity of *Og*ZnO NPs had absorbance degradation at 600 nm for methylene blue dye discoloration after 1 h, with a degradation maximum of 85%. In conclusion, the synthesized *Og*ZnO NPs could be used in several pharmaceutical and biotechnological applications.

Keywords: Bionanomaterial; Zinc Oxide Nanoparticles; *Ocimum gratissimum*; Antioxidant activity; Biotechnological applications

1.0 Introduction

Nanotechnology is a technology that involves development of nanomaterials for use in several industrial fields such as pharmaceutical, food processing, chemical and mechanical industries (Zeghoud *et al*., 2022). Nanotechnology plays an important role in the aspect of power generation, drug delivery, computing, optics and environmental sciences (Ramsden, 2016). Several nanoscale materials or devices have been developed through the nanotechnology using different methods, which include chemical, physical and green approaches. There are numerous downsides of conventional methodologies for the development and synthesis

of nanoparticles, including high cost of production, cumbersomeness of the techniques, long-term processing and specifically the utilization of toxic compounds. A large portion of the recent works and advances has been directed to fast processes and eco-friendlier techniques for the development of nanoparticles because of these constraints (Herlekar *et al*., 2014). In recent years, the development of environmentally friendly methods for synthesizing materials has been a major focus for researchers and scientists (Ilesanmi *et al*., 2021; Ilesanmi *et al*., 2023a). In this regard, biosynthesis of NPs, particularly utilizing extricates from various plants, is currently in vogue due to its simplicity, cost-effectiveness, and non-toxicity in green chemistry (Iravani, 2011).

Nanotechnology has also improved the standard of human activities by addressing numerous daily existence issues, such as energy adequacy, environmental change, material, textile and biomedicals including treatment of diseases such as Alzheimer's and cancers (Hasan, 2015). Because of their numerous applications in different specialized fields, thorough investigation on metal oxide nanoparticles has been deployed in the last decade. Among these, with multi-layered importance, ZnO NPs are highly invigorating inorganic materials. ZnO NPs can be utilized in different areas, like energy conservation, electronics, materials, semiconductors, medical services, catalysis, cosmetics and synthetic detection (Al-Naamani *et al*., 2016). The NPs are biocompatible, non-toxic and potentially exhibit remarkable biomedical applications, such as anti-cancer (Mishra *et al*., 2017), anti-inflammatory (Nagajyothi *et al*., 2015), anti-microbial, targeted drug delivery (Cai *et al*., 2016), wound healing, and bio-imaging (Gutha *et al*., 2017). Green synthesis of NPs involving the use of plant materials has previously been reported (Periasamy *et al*., 2016). Properties of extracts or materials differs remarkably in different media (Ilesanmi *et al*., 2014; Ilesanmi and Adewale, 2020). The unique and remarkable features of nanomaterials led to the emerging development of nanotechnology and nanoscience. Metal oxide nanoparticles have received more attention for several researches among other nanomaterials due to their high uniqueness in electrochemical coupling, non-toxicity, photostability, chemical stability, broad range of radiation absorption, low cost and easy availability (Liu, 2006). From in-depth comparison on metal oxide nanoparticles, zinc oxide (ZnO) nanoparticle is considered one of the foremost metal oxide nanomaterials owing to its physical, optical, chemical and biological properties (Salam and Sivaraj, 2014). ZnO NPs have been reported to have many applications in piezoelectric, optical, biomedical, mechanical, catalyst, gas sensing etc. (Kolodziejczak-Radzimska and Jesionowski, 2014).

Zinc oxide nanoparticles have been synthesized from various plant aqueous extracts such as *Moringa oleifera* (Elumalai *et al*., 2015), *Trifolium pratense* (Renata and Jolanta, 2016), *Passiflora caerulea* (Santhoshkumar *et al*., 2017), *Bauhinia tomentosa* (Sharmila *et al*., 2018), *Camellia sinensis* (Shagufta *et al*., 2018), *Azadirachta indica* (Handago *et al*., 2019), *Aloe vera* (Chaudhary *et al*., 2019), *Cinnamomum verum* (Mohammad *et al*., 2020), and *Lippia adoensis* (Demissie *et al*., 2020).

Scent leaf (*Ocimium gratissimum*) is a plant belonging to the herbaceous family Labiatae (Bhavani *et al*., 2019). It is an indigenous plant to tropical areas of West Africa and India. The plant is also available in the coastal and savannah areas especially in Nigeria. In India, the most commonly used names for the plant are Ram tulsi (Hindi), Vriddhutulsi (Sanskrit), Nimma tulasi (Kannada) (Bhavani *et al*., 2019). In the Southern western part of Nigeria, the plant is called "effinrin-nla". It is referred to as "Ahuji" by the Igbos, while it is known as "Daidoya" in the Northern part of Nigeria (Effraim *et al*., 2003).

Several methods have been reported for the synthesis of ZnO NPs, which include hydrothermal (Bharti and Bharati, 2017), processing of sol−gel (Savi *et al*., 2011), pyrolytic spraying (Widiyandari *et al*., 2018), precipitating analysis (Choy, 2003), deposition of chemical vapor (Yan *et al*., 2013), green synthesis, etc. Green synthesis among other methods is usually preferred because of its eco-friendliness, cost-effectiveness, novel properties, many applications

and non-toxicity of the synthesized materials for human pharmaceutical and therapeutic use (Donmez, 2020). Scent leaf (*Ocimum gratissimum*) has been reported to possess several phytochemicals that contributed to its medicinal applications (Bhavani *et al*., 2019). The phytochemicals in the aqueous extract of the plants act as a reducing and capping agent for the synthesis of nanoparticles (Zeghoud *et al*., 2022). However, *O. gratissimum* has not been exploited for synthesis of nanoparticles for various applications. Therefore, this work was aimed to synthesize ZnO NPs from *O. gratissimum* leaves extract and establish its potentials in pharmaceutical, environmental and biotechnological applications.

2. Materials and Methods

2.1 Collection and Preparation of Plant Material

This was carried according to the method of Sharmila and Gayathri (2014). Fresh leaves of *Ocimum gratissimum* were collected and thoroughly washed using distilled water and sun dried for residual moisture removal. The sun-dried leaves were thereafter grinded into fine powder and sieved with 150 μm pore size sieve. Five grams (5 g) of the fine powdered leaves were boiled in 100 ml of distilled water for 60 min at 100 ^{o}C with magnetic stirring at 800 rpm. The aqueous extract obtained was cooled to about 25 ^{o}C (room temperature) and subjected to filtration using Whatman No.1 filter paper. The extract was then stored at 4°C for further analyses.

2.2. Biosynthesis of Zinc Oxide Nanoparticles (ZnO NPs) from *O. gratissimum*

The biosynthesis of zinc oxide nanoparticles from the *O. gratissimum* leaf extract was carried out according to the method of Sharmila and Gayathri (2014). Briefly, 1:1 (50mL *O. gratissimum* extract and 50mL of 0.45M zinc acetate dihydrate), 3:2 (60mL *O. gratissimum* extract and 40mL of 0.45M zinc acetate dihydrate), and 9:1 (90mL *O. gratissimum* extract and 10mL of 0.45M zinc acetate dihydrate) ratios were added separately with 50 mL, 40 mL, and 10mL of 0.45M sodium hydroxide respectively. The three separate mixtures obtained were subjected to magnetic stirring at 800 rpm for 2 hr. This resulted to formation of yellow precipitate. The precipitates were removed with glass filter and washed with distilled water and ethanol in order to remove some of the impurities present. It was thereafter oven dried at 100°C for 1 hr and mashed using mortar and pestle. Finally, calcination of the mashed yellow powders was carried out at 400°C for 1 hr. The biosynthesized zinc oxide nanoparticles were subjected to further analyses and characterization.

2.3. Characterization of Biosynthesized *O. gratissimum* ZnO NPs

2.3.1. Thermal Gravimetric Analysis of *Og*ZnO NPs

Thermal gravimetric analysis of the synthesized ZnO NPs was carried out using a simultaneous DTA-TGA (DTG-60H, Shimadzu Co., Japan) analysis to analyze the decomposition and thermal stability of the biosynthesized ZnO NPs measured at the heating rate of 10°C/min.

2.3.2. X-ray Diffractometry Analysis of *Og*ZnO NPs

The mineral composition analysis of the *Og*ZnO NPs was carried out using XRD. X-ray powder diffractometry (p-XRD) measurements were performed on a Shimadzu XDS 2400H diffractometer with Cu anode control, 40 KV, 30 M.A, optics: Automatic divergence slit), in Bragg-Brentano configuration, using Cu-Kα radiation (1.54Å). The data were collected with 2θ value from 15° to 65°. The sample was inserted in a Lucite holder on the goniometer of the instrument which was designed with a graphite chromator. The XRD patterns of the sample were taken at 0°-60° 2θ range with a counting time of 14 s per step and size of 0.017°. The average size of the preparation was calculated using the Debye–Scherrer equation,

$D = (K\lambda)/\beta\cos\theta$, where λ represent the wavelength of the X-rays; β is the FWHM; K taken as Scherrer constant (0.9) and θ represents Bragg's angle in radians.

2.3.3. Scanning Electron Microscopy of *Og*ZnO NPs

The surface morphology and elemental composition of the biosynthesized *O. gratissimum* ZnO NPs were carried out by using scanning electron microscopy coupled with energy dispersive X-ray spectroscopy. Scanning electron microscopy (SEM, Hitachi SU 3500 scanning microscope, Tokyo, Japan) was employed to determine the shape of the produce samples. Particles were coated with gold un-der vacuum before SEM. The physical morphology of the sample surface and elemental composition was analyzed using Energy Dispersive X-ray Spectroscopy.

2.3.4 Fourier Transform Infra-red Spectrophotometric Analysis of *Og*ZnO NPs

The FTIR was carried out to investigate the progressions in the functional groups of the crude and carbonized test. The spectra were taken in the range of 4000 cm^{-1} to 500 cm^{-1}. The sample was prepared with potassium bromide at ration 1:100. Then, the mixture aws pressed to form a pellet of 13 mm. The pellet was thereafter inserted into the FTIR chamber for analysis. Potassium bromide served as reference material since it usually does not interfere in the infrared window from 400 to 4000 cm^{-1}.

2.3.5 UV-Vis Spectroscopic Analysis of *Og*ZnO NPs

The UV-Vis spectroscopic analysis was carried out on synthesized *Og*ZnO NPs and absorption spectra were recorded using JASCO UV-Vis spectroscopy (V-670) scanned in between a wavelength of 200 and 800 nm.

2.4. Antioxidant Activity of *Og*ZnO NPs

2.4.1 DPPH Radical Scavenging Activity Assay

A DPPH radical scavenging activity of the *Og*ZnO NPs was carried out according to the method of Rahman *et al*. (2022) to scavenge free radicals. Briefly it involved the combination of 2.4 ml 0.1 mM DPPH in methanol solution with 1.6 ml of extract in methanol at different concentrations of between 6.25 to 1200 µg ml^{-1}. The reaction mixture was incubated at 30 ºC for 30 min. The absorbance of the mixture was taken at 517nm. Ascorbic acid served as the standard. The percentage DPPH radical scavenging activity was thereafter estimated.

2.4.2 FRAP Radical Scavenging Activity of the Synthesized *Og*ZnO NPs

The antioxidant activity of *Og*ZnO NPs was estimated using FRAP assay according to the method reported by Gohari *et al.* (2011). A 2.7 ml of freshly prepared FRAP reagent (TPTZ, $FeCl_3$ and acetate buffer) at 37ºC was mixed with different concentration (200,500,1000µg/ml) of the synthesized nanoparticle and 270µl of distilled water. Using a blank containing FRAP reagent as reference, absorbance at 593 nm was determined at 10 min.

2.5. Photocatalytic Activity of *Og*ZnO NPs

Zinc oxide nanoparticles can potentially act as photocatalysts under the irradiation from sunlight. In this work, photocatalytic activity of the *Og*ZnO NPs was carried out according to the method of Rahman *et al*. (2022). Briefly, 50 mgl^{-1} solution of MB dye was used with a 0.25 mg/l of *Og*ZnO NPs. Both solutions were mixed together, and the blue dye solution was thereafter converted into a colorless solution within 1 h. The UV absorbance was taken at intervals of 0, 15, 30, 45 and 60 min. The percentage (%) degradation was calculated using the equation:

$$\% \text{ of degradation} = \left(\frac{C_i - C_f}{C_i}\right) \times 100$$

where the final and initial concentrations of the dye that degrade with time are expressed as C_f and C_i respectively.

3. Results

3.1 Zinc Oxide Nanoparticles Formation from *O. gratissimum*

There are several proposed mechanisms for the formation of ZnO NPs in the green synthesis approach. In this work, aqueous extract of *O. gratissimum* leaf were used as both the stabilizing, capping and reducing agent for ZnO NPs biosynthesis. The various phytochemicals present in *O. gratissimum* leaf are alkaloids, steroids, flavonoids, tannins, saponins, polyphenols

carbohydrates and reducing sugars (Bhavani *et al*., 2019). The metabolites or phytochemicals in *O. gratissimum* leaf are essential for the NPs preparation, acting as the capping and reducing agents. It is proposed that the ZnO NPs was formed by interaction and attachment of aromatic hydroxyl (OH) groups in the polyphenols and phytochemicals with the Zn^{2+} ions from zinc acetate dihydrate resulting into a stable complex system. ZnO NPs was released from the complex system during centrifugation and calcination.

Table 1: XRD Diffraction Pattern of the Synthesized *Og*ZnO NPs

Peak	2θ/degree	Plane	Intensity	d-Valve (A˚)	Minerals	Compositions (wt%)
1	22.98	1 0 0	56.14	3.8670	Wurtzite	19.90
2	25.12	0 0 2	52.47	3.5424	Wurtzite	28.80
3	27.00	1 0 1	69.21	3.2996	Wurtzite	37.99
4	37.01	1 0 2	24.33	2.4269	Wurtzite	13.36
5	45.10	1 1 0	26.48	2.0086	Wurtzite	14.54
6	50.97	1 0 3	26.46	1.7904	Wurtzite	14.52
7	54.00	2 0 0	4.32	1.6967	Wurtzite	2.37
8	55.57	1 1 2	14.15	1.6525	Wurtzite	7.77
9	57.00	2 0 1	8.61	1.6144	Wurtzite	4.72

3.2. Thermogravimetric (TGA) and Differential Thermal (DTA) Analyses of the *Og*ZnO NPs

Both TGA and DTA analyses were carried out on the *Og*ZnO NPs. The TGA and DTA curves demonstrated mass loss of the sample and energy change respectively during the process (Figure 1). TGA/DTA transition revealed a loss of 12.65% up to 650°C, however, at up to 1000°C, no considerable loss in mass was observed. This is an indication that the *Og*ZnO NPs are thermally stable after 650°C.

3.3. X-Ray Diffraction (XRD) Analysis of the Synthesized *Og*ZnO NPs

Figure 2 shows the XRD pattern of ZnO nanoparticles synthesized using zinc acetate dihydrate and *O. gratissimum* leaf extract. The peaks diffracted appeared at a 2θ value of ≈22.98°, 25.12°, 27.00°, 37.01°, 45.10°, 50.97°, 54.00°, 55.57°, and 57.00° corresponding to (100), (002), (101), (102), (110), (103), (200), (112), and (201) crystal planes, respectively (Table 1). Orthogonal phases (crystalline) were indicated by the XRD patterns. After the scanning of the sample, mineral peaks were thereafter identified.

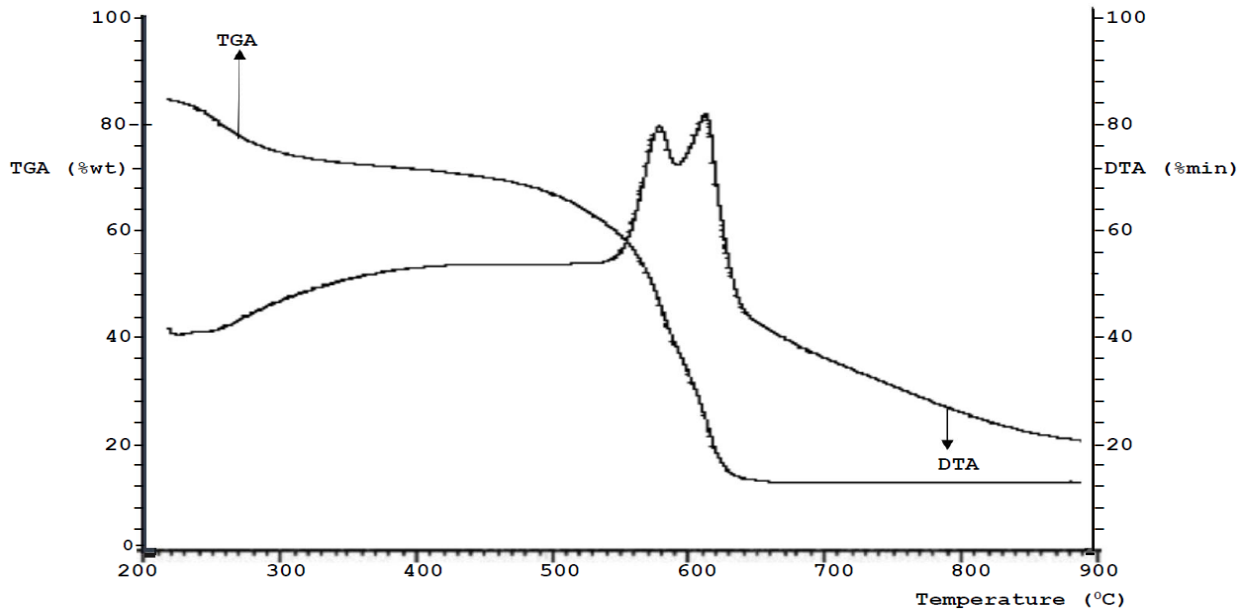

Figure 1: Thermal (TGA-DTA) analysis of the synthesized *O. gratissimum* ZnO NPs

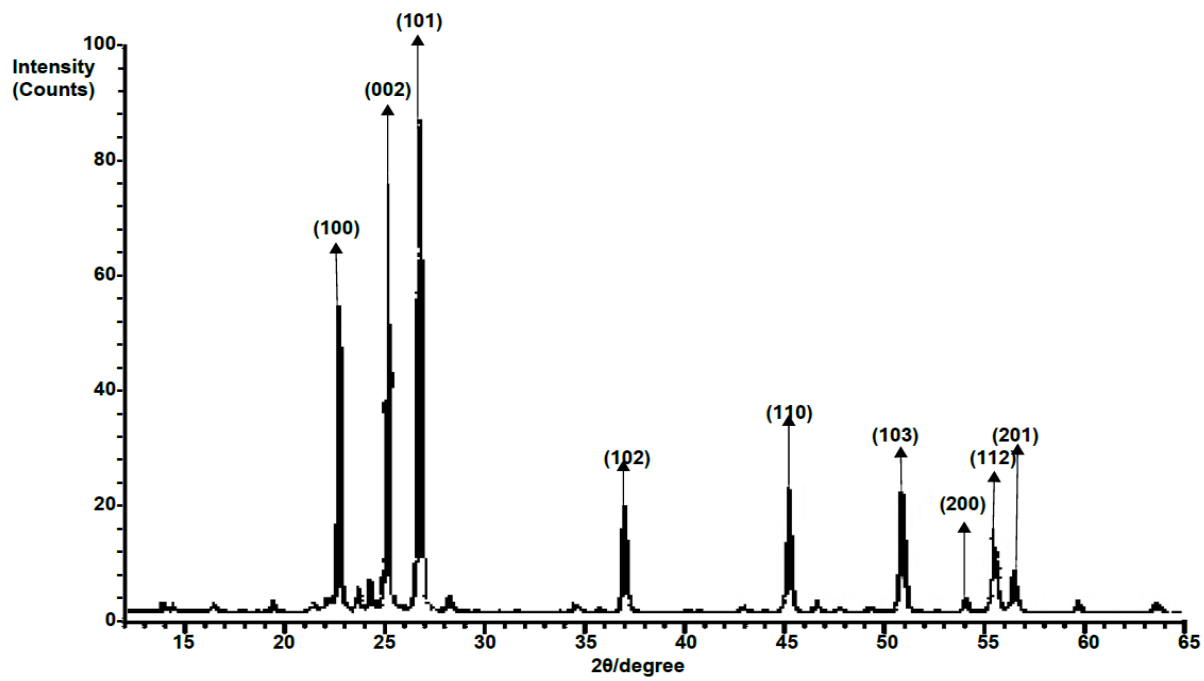

Figure 2: XRD pattern of the synthesized *O. gratissimum* ZnO NPs

3.4. FTIR Analysis of *Og*ZnO NPs

The FTIR analysis of the synthesized *Og*ZnO NPs are as shown in Figure 3. Different bands were observed at 3246 cm^{-1}, 2921 cm^{-1}, 2522 cm^{-1}, 1892 cm^{-1}, 1217 cm^{-1}, 1043 cm^{-1} and 650 cm^{-1} for the *Og*ZnO nanoparticles, respectively. A broad peak was observed at around 3246 due to O-H stretching vibration due to absorbed water. Absorption bands at 2522 is because of the presence of C-H stretching vibrations.

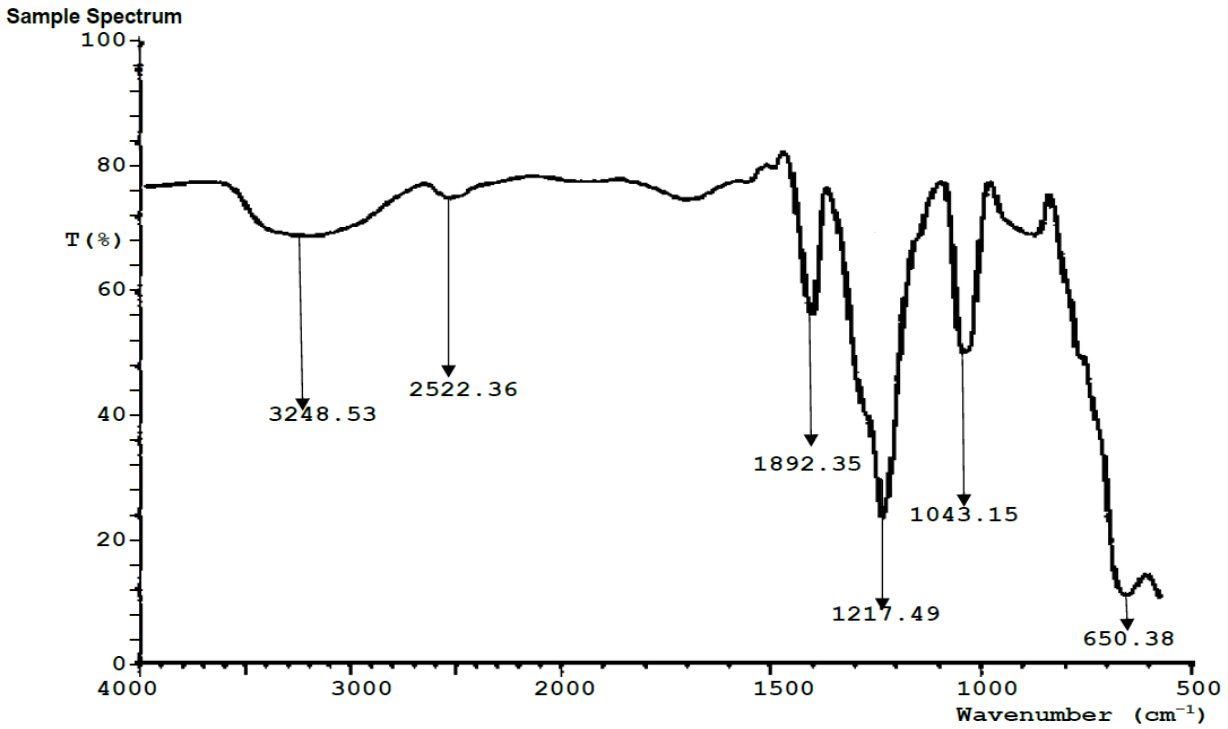

Figure 3: FTIR spectra of the synthesized *O. gratissimum* ZnO NPs

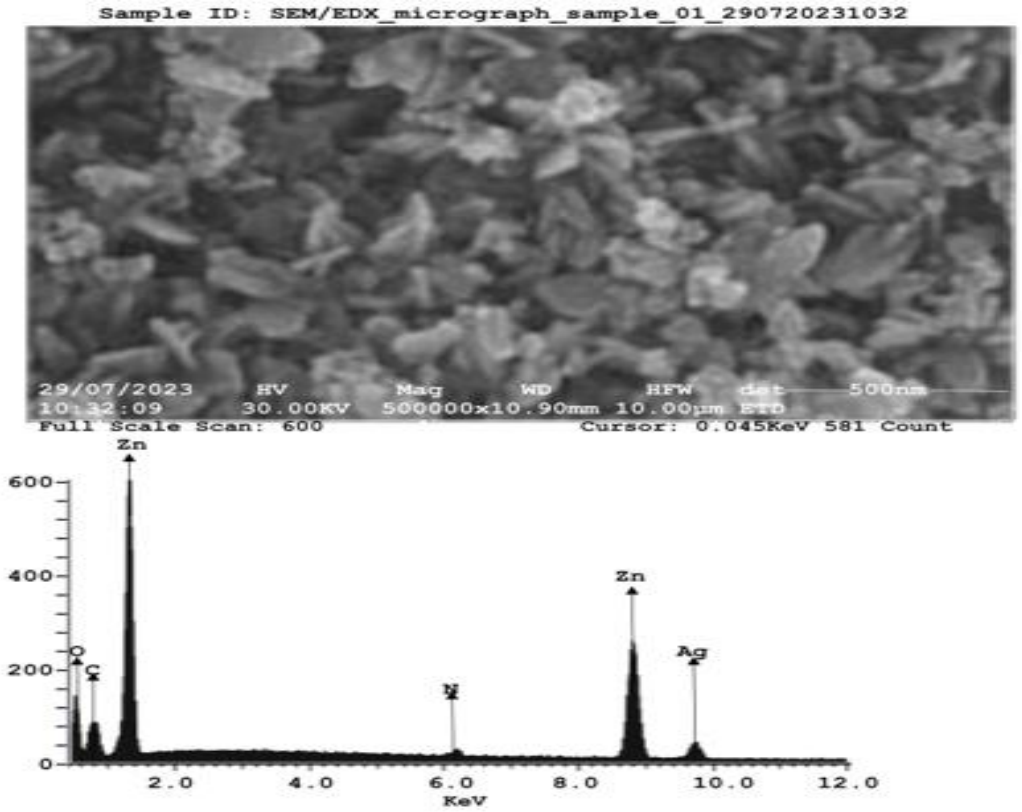

Figure 4: SEM images and EDX spectra of the synthesized *O. gratissimum* ZnO NPs

The peak at around 1892 cm^{-1} is due to the C=O stretching vibration of carbonyl group, whereas 1217 cm^{-1} was as a result of C-O stretching and the intensity at 1043 cm^{-1} is due to C-C stretching of cycloalkanes. The peak in the region of 650 cm^{-1} is typical of Zn-O stretching confirming the synthesis of ZnO NPs from *O. gratissimum* extract used as a capping and reducing agent.

3.5. SEM-EDS Analyses of the Synthesized *Og*ZnO NPs

SEM analysis revealed the surface morphologies of the synthesized *Og*ZnO NPs as presented in Figure 4. The SEM image shows triangular shapes inclined together as a result of the capping agent that stabilizes the materials. The EDX spectrum confirms the presence of carbon and oxygen. It also revealed the agglomeration of the particles with narrow particle size distributions with 79.32 nm and a height of 6.14 mm. The percentage elemental composition of the synthesized nanoparticles is 17.86%, 21.75%, 58.28%, 0.62% and 0.48% for carbon, oxygen, zinc, silver and nitrogen respectively.

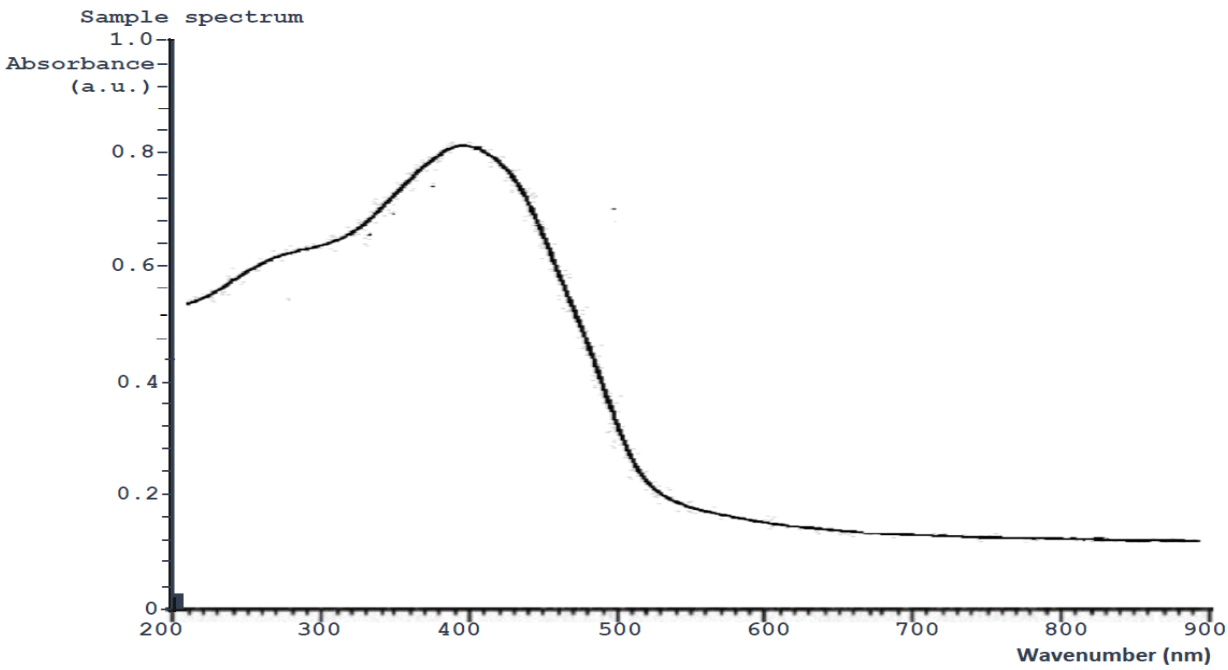

Figure 5: UV-Vis absorbance spectra of *O. gratissimum* ZnO NPs

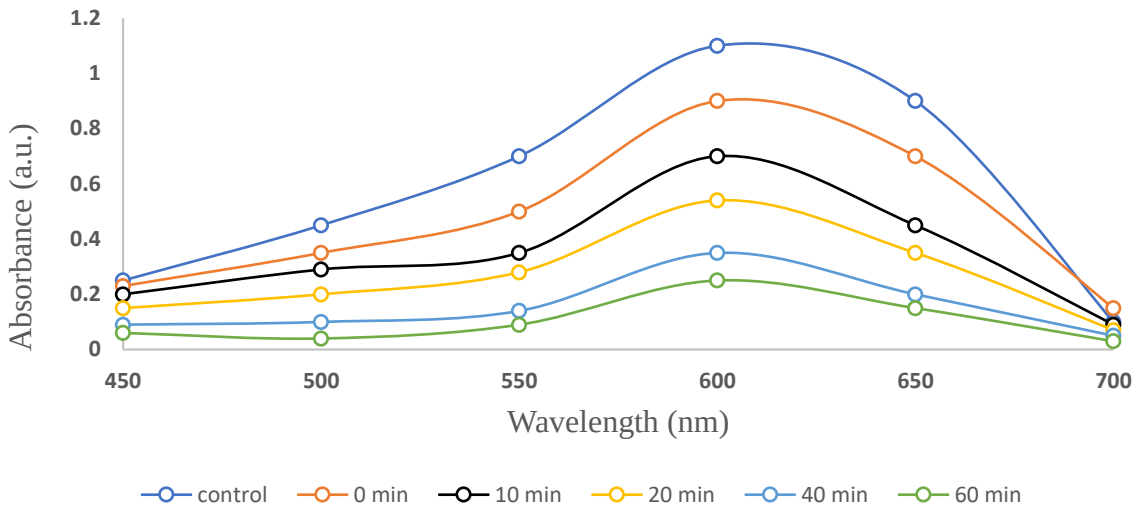

Figure 6: UV–Vis spectra for degradation of MB dye through the photocatalytic activity of the synthesized *O. gratissimum* ZnO NPs

3.6 UV-Vis Spectral Analysis of the Synthesized *Og*ZnO NPs

UV-Vis absorption spectra of the synthesized *Og*ZnO NPs is as shown in Figure 5. The strong absorption bands obtained in the range of 350–400nm corresponds to the characteristic band of ZnO nanoparticles. The purity of the ZnO NPs is confirmed by absence of any other peak in the spectra.

3.7 Antioxidant Activity of the Synthesized *Og*ZnO NPs

The FRAP activity of the synthesized *Og*ZnO NPs was demonstrated. After 10 minutes of incubation period, the pattern of absorbance obtained at 593nm for various concentrations (200, 500, 1000µg/ml) of the synthesized nanoparticles revealed that it possesses antioxidant property in a concentration dependent manner.

3.8 Photocatalysis of the Synthesized *Og*ZnO NPs

Photocatalytic activity of the synthesized *Og*ZnO NPs is as shown in Figure 6. The final absorbance obtained by mixture of *Og*ZnO NPs with the dye was compared to the initial absorbance of the dye. It was revealed that the absorbance degrades at 600 nm. The dye and *Og*ZnO NPs preparation was discolored after 1 h. The degradation of the MB dye by *Og*ZnO NPs was 85%.

4. Discussion

Nanobiotechnology as a branch of material science has recently gained attention and remarkable trend by researchers in the field of nanomaterial science and technology. Because of its unique properties and large variety of applications, the field has currently stood out of numerous global researches. Bionanomaterials are usually prepared using various methods such as chemical, physical and biological techniques. There are different reported methods of metal oxide nanoparticles production even in biological systems, including fungi, yeasts, bacteria, viruses, actinomycetes, and plants (Zeghoud *et al*., 2022). Among these methods, zinc oxide nanoparticles (ZnO NPs) obtained from plant-derived materials, appears to be more successful scheme to create a rapid, biocompatible, non-toxic, and ecofriendly platform for the synthesis and utilization of these bionanomaterials (Zeghoud *et al*., 2022). Different plant leaves such as bitter leaf, moringa, scent leaf etc. had been reported to possess several phytochemicals/polyphenols that contributed to its several applications (Bhavani *et al*., 2019;

Ilesanmi and Adedugbe, 2023; Ilesanmi *et al*., 2023b).

In this work, green synthesis of zinc oxide nanoparticles was done using *O. gratissimum* leaf aqueous extract as capping, reducing, and stabilizing agents. The synthesis involved processes leading to discoloration of the mixture from light brown to dark gray, which ascertained zinc oxide nanoparticles formation (Jan *et al*., 2020). The synthesized *Og*ZnO NPs was subjected to morphological and physicochemical characterizations for suitability in various applications. It has been earlier reported that characteristics of ZnO NPs highly dependent on the plant species, the reaction conditions of reaction such as temperature, pH and synthesis medium (Guilger-Casagrande and de Lima, 2019).

FTIR spectroscopy was employed to identify the functional groups present in the synthesized *O. gratissimum* zinc oxide nanoparticles (*Og*ZnO NPs). This was performed in the range of 4000−400 cm^{-1}. The peak of ZnO obtained at 650 cm^{-1} could be due to zinc and oxygen bonding vibrations (Nimbalkar and Patil, 2017). Also, the spectra exhibited broad peak at 3246 due to O-H stretching vibration due to absorbed water. Absorption bands at 2522 is because of the presence of C-H stretching vibrations. The peak at around 1892 cm^{-1} is due to the C=O stretching vibration of carbonyl group, whereas 1217 cm^{-1} was as a result of C-O stretching and the intensity at 1043 cm^{-1} is due to C-C stretching of cycloalkanes. The peak in the region of 650 cm^{-1} is assigned to Zn-O stretching vibration confirming ZnO NPs are synthesized using *O. gratissimum* extract as a reducing and capping agent. The peak at 900 cm^{-1} is assigned to phosphodiester stretching of glycogen having a strong binding ability with zinc. The binding created a layer on its surface that prevented agglomeration in the reaction medium (Lu *et al*., 2019; Kim *et al*., 2019).

The X-ray diffraction pattern of zinc oxide nanoparticles shows definite line broadening of the X-ray diffraction peaks, showing that the prepared particles were in the nanoscale range. The peaks diffracted at a 2θ value of ≈22.98°, 25.12°, 27.00°, 37.01°, 45.10°, 50.97°, 54.00°, 55.57°, and 57.00° that corresponded to crystal planes of (100), (002), (101), (102), (110), (103), (200), (112), and (201) respectively. The XRD patterns indicated crystalline orthogonal phases. After the X-ray scanning of the samples, mineral peaks were identified using Software. The background and peak-positions were identified and based on the peak positions and intensities (Zhou *et al*., 2007; Khoshhesab *et al*., 2011). All the characteristic peaks obtained revealed the synthesized ZnO NPs with no impurities. The size of the zinc oxide particles was calculated with Debye−Scherrer formula. On the bases of Bragg's diffraction angle (θ) and full width at half-maximum (β) of intense peaks that corresponding to 101 planes in position located at 36.2°, the particle size is about 29 nm (Kaskow *et al*., 2018), while the average particle size is 41.23 nm. This confirms the standard orthogonal wurtzite structure of ZnO-NPs as reported in the previous studies (Arakha *et al*., 2015).

Thermal gravimetric analysis (TGA) spectra obtained for the *Og*ZnO NPs indicated that the sample thermally decomposed with increasing temperature values. TGA and DTA curves show mass loss and change in energy of the sample during the process. TGA/DTA transition shows a loss of 12.65% up to 650°C, with no change in mass at temperature up to 1000°C. In-depth analysis shows that the biosynthesized *Og*ZnO NPs is thermally stable after 650°C. The mass loss and energy change may probably be due to the presence of volatile components in the plant sample. Similar weight loss was also reported by Fatimah *et al*. (2016) for ZnO NPs obtained from leaf extracts of *Mimosa pudica*.

Scanning electron microscopy (SEM) was used to study the morphological study of the green synthesized zinc oxide nanoparticles (Rajiv *et al*., 2013). The particles show triangular shape, and these particles are in a highly agglomerated form. The EDX spectrum confirms the presence of carbon and oxygen. It also revealed the agglomeration of the particles with narrow particle size distributions with 79.32 nm and a height of 6.14 mm. The percentage elemental composition of the synthesized nanoparticles is

17.86%, 21.75%, 58.28%, 0.62% and 0.48% for carbon, oxygen, zinc, silver and nitrogen respectively. Increase in size may be due to overlapping of particles on each other. The formation of ZnO-NPs was established by comparison of the particle size obtained by XRD and SEM analyses. Our results were in agreement with previous reports (Pillai *et al*., 2020). The result of EDX revealed clearly that there is synthesis and/or formation of zinc oxide nanoparticles.

Antioxidant activity of the synthesized ZnO nanoparticles was investigated using FRAP method. The synthesized molecule demonstrated high free radical scavenging activity. The antioxidant properties of ZnO nanoparticles are based on the account of the electron density transfer at the oxygen atoms (Stan *et al*., 2016). The normally developed material exhibits a critical regular cell reinforcement activity from higher plants against persistent issues brought about by oxidative processes. Zinc has the potentials to attack free radicals by ameliorating the cell membrane damage. Zinc is an important cofactor for several enzymes and a component in the oxidative processes. Antioxidant enzymes preserves mitochondrial membrane structure from damages by eliminate radicals in the body (Zhao *et al*., 2014).

The photocatalytic behavior of the synthesized nanoparticles was demonstrated. The dye degradation potential was established in a concentration dependent manner with respect to time. One possible explanation to the photocatalytic mechanism employed by the biosynthesized nanoparticles is through the production of reactive oxygen species by hydroxyl radical generation (photo-oxidation) and peroxide radical generation (photo-reduction) processes (Osuntokun *et al*., 2019). The reactive oxygen species generated degraded the dye into carbon dioxide, mineral acids and water (Lua *et al*., 2019).

5.0 Conclusion

In this study, we have successfully synthesized ZnO NPs with an average size of 16.6 nm, using scent leaf (*O. gratissimum*) extract by green approach which is more advantageous over chemical method. The synthesized *Og*ZnO NPs was characterized by different methods of analysis, such as SEM, XRD, TGA, EDX, FTIR and UV–Vis spectroscopic analyses. The aqueous solution of the nanomaterial showed maximum absorption (λmax), at 400 nm. The XRD patterns of the *Og*ZnO NPs indicated crystalline orthogonal wurtzite structure. Reducing biomolecules responsible for the stabilization and encapsulation of the nanoparticles was revealed by functional groups identified by the FTIR analysis. In addition, the elemental composition from EDX analysis confirms the ZnO NPs formation. The antioxidant study of the synthesized *Og*ZnO NPs showed moderate activity against various free radicals. Thus, it was concluded that the synthesized ZnO NPs could be of interest in pharmaceutical, biomedical, cosmetics and biotechnological applications, and possibly in environmental remediation as photocatalysts in several dye degradation processes.

CRediT Authorship Contribution Statement

All authors equally contribute to Conceptualization, Methodology, Formal analysis, Investigation, Writing, and Visualization

Declaration of Competing Interest

The author declares no known competing interests that could have appeared to influence the work reported in this paper.

Data Availability

Data will be made available on request.

Acknowledgements

The author acknowledges the support of Ms. L. O. Ogunlade of the Biochemistry Laboratory of Achievers University and the support of the institution.

References

Al-Naamani, L., Dobretsov, S. and Dutta, J. (2016). Chitosan-zinc oxide nanoparticle composite coating for active food packaging applications. *Innovative Food Sci. Emerging Technol.* 38:231−237.

Arakha, M., Saleem, M., Mallick, B.C. and Jha, S. (2015). The effects of interfacial potential on antibacterial activity of zinc oxide nanoparticles derived from *Bauhinia tomentosa* leaf extract. *Journal of Nanostructure in Chemistry* 8:293–299.

Bharti, D.B. and Bharati, A.V. (2017). Synthesis of ZnO nanoparticles using a hydrothermal method and a study its optical activity. *Luminescence* 32:317–320.

Bhavani, T., Mohan, R.R., Mounica, C., Nyamisha, J., Krishna, A.G., Prabhavathi, P., Raja, R.R. and Baba, K.H. (2019). Phytochemical screening and antimicrobial activity of *Ocimum gratissimum* review. *Journal of Pharmacognosy and Phytochem.* 8:76-79.

Cai, X., Luo, Y., Zhang, W., Du, D. and Lin, Y. (2016). pH-Sensitive ZnO quantum dots doxorubicin nanoparticles for lung cancer targeted drug delivery. *ACS Appl. Mater. Inter.* 8:22442−22450.

Chaudhary, A., Kumar, N., Kumar, R. and Kumar, R. (2019). Antimicrobial activity of zinc oxide nanoparticles synthesized from *Aloe vera* peel extract. *SN Applied Sciences* 1:136.

Choy, K.L. (2003). Chemical vapour deposition of coatings. *Progress in Materials Sci.* 48:57– 170.

Demissie, M.G., Sabir, F.K., Edossa, G. D. and Gonfa, B. A. (2020). Synthesis of zinc oxide nanoparticles using leaf extract of *Lippia adoensis* (Koseret) and evaluation of its antibacterial activity. *Journal of Chemistry* 7459042.

Dönmez, S. (2020). Green synthesis of zinc oxide nanoparticles using *Zingiber officinale* root extract and their applications in glucose biosensor. *El-Cezeri Fen ve Mühendislik Dergisi* 7:1191–1200.

Effraim, K.D., Jacks, T.W. and Sodipo, O.A. (2003). Histopathological studies on the toxicity of *Ocimum gratissimum* leave extract on some organs of rabbit. *Afr J Biomed Res.* 6:21-25.

Elumalai, K., Velmurugan, S., Ravi, S., Kathiravan, V. and Ashokkumar, S. (2015). Green synthesis of zinc oxide nanoparticles using *Moringa oleifera* leaf extract and evaluation of its antimicrobial activity. *Spectrochimica Acta Part A: Molecular and Biomolecular Spectros.* 143:158–164.

Fatimah, I., Pradita, R.Y. and Nurfalinda, A. (2016). Plant extract mediated of ZnO nanoparticles by using ethanol extract of *Mimosa pudica* leaves and coffee powder. *Procedia Eng.* 148:43−48.

Gohari, A.R., Hajimehdipoor, H., Saeidnia, S. Ajani, Y. and Hadjiakhoondi, A. (2011). Antioxidant activity of some medicinal species using FRAP assay. *Journal of Medicinal Plants* 10:54-60.

Guilger-Casagrande, M. and de Lima, R. (2019). Synthesis of silver nanoparticles mediated by fungi: A review. *Front. Bioeng. Biotechnol.* 7:287.

Gutha, Y., Pathak, J.L., Zhang, W., Zhang, Y. and Jiao, X. (2017). Antibacterial and wound healing properties of chitosan/poly (vinyl alcohol)/zinc oxide beads (CS/PVA/ZnO). *Int. J. Biol Macromol*. 103:234−241.

Handago, D. T., Enyew, A. Z. and Bedasa, A. G. (2019). Effects of *Azadirachta indica* leaf extract, capping agents, on the synthesis of pure and Cu doped ZnO-nanoparticles: a green approach and microbial activity. *Open Chemistry* 17:246–465.

Hasan, S. (2015). A review on nanoparticles: their synthesis and types. *Res. J. Recent Sci.* 4:1−3.

Herlekar, M., Barve, S. and Kumar, R. (2014). Plant-mediated green synthesis of iron nanoparticles. *Journal of Nanopart.* 140614.

Ilesanmi, O. S., Ojopagogo, Y. A. and Adewale, I. O. (2014). Kinetic characteristics of purified tyrosinase from different species of *Dioscorea* (Yam) in aqueous and non-aqueous systems. *Journal of Molecular Catalysis B: Enz.* 108:111-117.

Ilesanmi, O. S. and Adewale, I. O. (2020). Physicochemical properties of free and immobilized tyrosinase from different species of yam (*Dioscorea* spp). *Biotechnology rep.* e00499.

Ilesanmi, O.S., Adedugbe, O.F. and Adewale, I.O. (2021). Potentials of purified tyrosinase from yam (*Dioscorea* spp) as a biocatalyst in the synthesis of cross-linked protein networks. *Heliyon* 7:e07831.

Ilesanmi, O.S. and Adedugbe, O. F. (2023). Novel peroxidase from bitter leaf (*Vernonia amygdalina*): purification, biochemical characterization and biotechnological applications. *Biocatal. Agric. Biotechnol.* 49:102662.

Ilesanmi, O. S., Adedugbe, O. F., Oyegoke, D. A., Olagunju, V. A. and Adewale, I. O. (2023a). Synthesis of organic compounds using yellow yam (*Dioscorea praehensilis*) tyrosinase as catalyst. *African Journal of Pharmacy and Pharmacol.* 17:136-147.

Ilesanmi, O. S., Adedugbe, O. F., Oyegoke, D. A., Adebayo, R. F. and Agboola, O. E. (2023b). Biochemical properties of purified polyphenol oxidase from bitter leaf (*Vernonia amygdalina*) Heliyon 9: e17365.

Iravani, S. (2011). Green synthesis of metal nanoparticles using plants. *Green Chem.* 13:2638−2650.

Jan, H., Shah, M., Usman, H., Khan, A., Muhammad, Z., Hano, C. and Abbasi, B. H. (2020). Biogenic synthesis and characterization of antimicrobial and anti-parasitic zinc oxide (ZnO) nanoparticles using aqueous extracts of the himalayan columbine (*Aquilegia pubiflora*). *Front. Mater.* 7:249.

Kaskow, I., Decyk, P. and Sobczak, I. (2018). The effect of copper and silver on the properties of Au-ZnO catalyst and its activity in glycerol oxidation. *Appl. Surf. Sci.* 444:197−207.

Khoshhesab, Z. M., Sarfaraz, M. and Asadabad, M. A. (2011). Preparation of ZnO nanostructures by chemical precipitation method. *Synth. React. Inorg., Met.-Org., Nano- Met. Chem.* 41: 814−819.

Kim, W.J., Soshnikova, V., Markus, J., Oh, K. H., Anandapadmanaban, G., Mathiyalagan, R., Kołodziejczak-radzimska, A. and Jesionowski, T. (2014). Zinc oxide —from synthesis to application: a review. *Materials* 7:2833–2881.

Liu, W. T. (2006). Nanoparticles and their biological and environmental applications. *Journal of Bioscience and Bioeng.* 102:1–7.

Lu, J., Batjikh, I., Hurh, J., Han, Y., Ali, H., Mathiyalagan, R., Ling, C., Ahn, J.C. and Yang, D.C. (2019). Photocatalytic degradation of methylene blue using biosynthesized zinc oxide nanoparticles from bark extract of *Kalopanax septemlobus. Optik.* 182:980−985.

Lua, J., Batjikh, I., Hurh, J., Han, Y., Ali, H., Mathiyalaganb, R., Ling, C., Ahn, C.J. and Yang, D.C. (2019). Photocatalytic degradation of methylene blue using biosynthesized zinc oxide nanoparticles from bark extract of *Kalopanax septemlobus. Inter J. Light Electron Optics* 182:980–985.

Mishra, P.K., Mishra, H., Ekielski, A., Talegaonkar, S. and Vaidya, B. (2017). Zinc oxide nanoparticles: a promising nanomaterial for biomedical applications. *Drug Discovery Today* 22:1825−1834.

Mohammad, A.A., Mahadevamurthy, M. and Daruka, P. (2020). *Cinnamomum verum* bark extract mediated green synthesis of ZnO nanoparticles and their antibacterial potentiality. *Biomolecules* 10:134–336.

Nagajyothi, P., Cha, S.J., Yang, I.J., Sreekanth, T., Kim, K.J. and Shin, H. M. (2015). Antioxidant and anti-inflammatory activities of zinc oxide nanoparticles synthesized using *Polygala tenuifolia* root extract. *J. Photochem. Photobiol. B* 146:10−17.

Nimbalkar, A. R. and Patil, M. G. (2017). Synthesis of ZnO thin film by sol-gel spin coating technique for H_2S gas sensing application. *Physica B.* 527:7−15.

Osuntokun, J., Onwudiwe, D.C. and Ebenso, E.E. (2019). Green synthesis of ZnO nanoparticles using aqueous *Brassica oleracea* L. var. italica and the photocatalytic activity. *Green Chem. Lett. Rev.* 12:444–457.

Perez, Z.E.J., Kim, Y.J. and Yang, D.C. (2019). Room temperature synthesis of germanium dioxide nanorods and their in vitro photocatalytic application. *Optik.* 178:664−668.

Periasamy, G., Karim, A., Gibrelibanos, M. and Gebremedhin, G. (2016). Nutmeg (*Myristica fragrans* Houtt.) oils. In Essential Oils in Food Preservation, Flavor and Safety; *Elsevier* 607−616.

Pillai, A.M., Sivasankarapillai, V.S., Rahdar, A., Joseph, J., Sadeghfar, F., Rajesh, K. and Kyzas, G.Z. (2020). Green synthesis and characterization of zinc oxide nanoparticles with antibacterial and antifungal activity. *J. Mol. Struct.* 1211:128107.

Rahman, F., Majed Patwary, M.A., Bakar Siddique, M.A., Bashar, M.S., Haque, M.A., Akter, B., Rashid, R., Haque, M.A. and Royhan Uddin, A.K.M. (2022). Green synthesis of zinc oxide nanoparticles using *Cocos nucifera* leaf extract: characterization, antimicrobial, antioxidant and photocatalytic activity. *R. Soc. Open Sci.* 9:220858.

Rajiv, P., Rajeshwari, S. and Venckatesh, R. (2013). Bio-Fabrication of zinc oxide nanoparticles using leaf extract of *Parthenium hysterophorus* L. and its size-dependent antifungal activity against plant fungal pathogens. *Spectrochim. Acta, Part A.* 112:384−387.

Ramsden, J. (2016). Nanotechnology: An Introduction; William Andrew, 2016.

Renata, D. and Jolanta, D. (2016). Biosynthesis and antibacterial activity of ZnO nanoparticles using *Trifolium pratense* flower extract. *Saudi Journal of Biological Sci.* 23:517–523.

Salam, H.A. and Sivaraj, R. (2014). Green synthesis and characterization of zinc oxide nanoparticles from *Ocimum basilicum* L. *Var. purpurascens* Benth.-Lamiaceae leaf extract. *Materials Lett.* 131:16–18.

Santhoshkumar, J., Kumar, S.V., Rajeshkumar, S. and Adaikalaraj, G. (2017). Synthesis of zinc oxide nanoparticles using plant leaf extract against urinary tract infection pathogen. *Resource Efficient Technol.* 3:459–1651.

Savi, B.M., Rodrigues, L. and Bernardin, A.M. (2011). Synthesis of ZnO nanoparticles by Sol−Gel processing. Santa Catarina Extreme South University, 1–8.

Shagufta, I., Amna, S. and Aftab, A.A. (2018). Green tea leaves mediated ZnO nanoparticles and its antimicrobial activity. *Cogent Chemistry* 4:1469207.

Sharmila, D.R. and Gayathri, R. (2014). Green synthesis of zinc oxide nanoparticles by using *Hibiscus rosa-sinensi*. *International Journal of Current Engineering and Technol.* 4:1137.

Sharmila, G., Muthukumaran, C. and Sandiya, K. S. (2018). Biosynthesis, characterization, and antimicrobial propensity of ZnO nanoparticle. *Sci. Rep.* 5:9578.

Stan, M., Popa, A., Toloman, D., Silipas, T. D. and Vodnar, D. C. (2016). Antibacterial and antioxidant activities of ZnO nanoparticles synthesized using extracts of *Allium sativum*, *Rosmarinus officinalis* and *Ocimum basilicum. Acta Metall. Sin. (Engl. Lett.)* 29:228–236.

Widiyandari, N., Umiati, A.K. and Herdianti, R.D. (2018). Synthesis and photocatalytic property of zinc oxide (ZnO) fine particle using flame spray pyrolysis method. *Journal of Physics:Conference Series* 1025, 012004.

Yan, K., Fu, L., Peng, H. and Liu, Z. (2013). Designed CVD growth of graphene via process engineering. *Accounts of Chemical Res.* 46:2263–2274.

Zeghoud, S., Hemmami, H., Seghir, B. B., Amor, I. B., Kouadri, I., Rebiai, A., Messaoudi, M., Ahmed, S., Pohl, P. and Simal-Gandara, J. (2022). A review on biogenic

green synthesis of ZnO nanoparticles by plant biomass and their applications. *Materials Today Communications* 33:104747.

Zhao, C.Y., Tan, S.X., Xiao, X.Y., Qiu, X.S., Pan, J.Q. and Tang, Z.X. (2014). Effects of dietary zinc oxide nanoparticles on growth performance and antioxidative status in broilers. *Biol. Trace Elem. Res.* 160:361–367.

Zhou, J., Zhao, F., Wang, Y., Zhang, Y. and Yang, L. (2007). Size-controlled synthesis of ZnO nanoparticles and their photoluminescence properties. *J. Lumin.* 122−123:195−197.